Navier-Stokes Solutions for Flow Past a Class of Two-Dimensional Semi-Infinite Bodies

U. GHIA* AND R. T. DAVIS†
University of Cincinnati, Cincinnati, Ohio

The complete Navier-Stokes equations have been used to analyze the symmetric laminar incompressible flow past a class of two-dimensional semi-infinite bodies including the family of parabolas and rectangular slabs as special cases. The problem is formulated in terms of coordinates obtained from the Cartesian coordinates by a conformal transformation. Similarity-type variables are used for the vorticity and stream functions. In these variables, the solution approaches the Blasius solution far downstream and the correct inviscid flow transversely far from the body surface. The formulation also produces the correct starting solution along the stagnation streamline. An alternating direction implicit finite-difference method is used to obtain the numerical solution. Results are presented for the skin-friction function and the surface pressure distributions for various values of the problem parameters. For the rectangular slab with a sharp shoulder, the wall shear is unbounded at the shoulder; however, the vorticity function employed remains bounded. For large Reynolds number, separation and reattachment are observed aft of the region of the shoulder, resulting in a separation bubble of finite, sometimes quite large extent. The flow structure in the separation region is carefully analyzed. Finally, it is shown that a certain boundary-layer-type simplified form of the vorticity equation may be used in separation studies if the displacement effects are correctly accounted for through the complete stream function equation.

I. Introduction

IT is desirable to use the complete Navier-Stokes equations in order to describe a flowfield accurately. The resulting solution is then uniformly valid in the entire flowfield. However, the difficulties associated with solution of these nonlinear partial differential equations are well known. Analytical solutions are impossible for all but the simplest flows where the equations reduce to a considerably simpler form. Approximate methods of solution are generally based on simplifying assumptions regarding the vorticity transport process or about the viscous diffusion and the pressure field. The solutions thus obtained are valid only in those regions of the flow where the assumptions underlying the solutions remain valid. One exception to this is the boundary-layer solution obtained in optimal coordinates; for unseparated boundary layers, this solution remains uniformly valid in the entire flowfield.

The present high-speed, large storage, digital computers have now made it possible to solve the Navier-Stokes equations without these simplifying assumptions. Many researchers have pursued this direction. While these solutions are uniformly valid, the computer time required to obtain these solutions can become excessive for nonsimple geometry of the problem. Efforts have also been made to overcome this difficulty by developing efficient numerical schemes while simultaneously developing better mathematical formulations of the flow problem. Among this class of solutions are the results obtained by Davis,[1] Davis and Werle,[2] and Davis, U. Ghia, and K. N. Ghia[3,4] for the flow past parabolic cylinders, paraboloids of revolution, and blunted and sharp wedges.

The present paper represents a general and useful formulation of the Navier-Stokes equations for a class of laminar incompressible flows. The problem is expressed in terms of general conformal coordinates which reduce to the second-order optimal coordinates for the corresponding nonseparated boundary-layer flow past the semi-infinite thin flat plate. Similarity-type vorticity and stream functions are used as the dependent variables in the Navier-Stokes equations. The equations are then solved by an alternating direction implicit finite-difference scheme to determine the symmetric flow past two-dimensional semi-infinite bodies of the form shown in Fig. 1 by the curves of $\eta = \text{const}$. For this geometry, the conformal coordinates used are obtained from the Cartesian coordinates by a Schwarz-Christoffel transformation. Results are presented for the skin friction and the surface pressure for several values of the Reynolds number and the bluntness of the body shoulder. As this bluntness approaches zero, the skin friction and the surface pressure gradient become unbounded at the sharp shoulder. However, the vorticity function used in the present formulation remains bounded even at the sharp shoulder. The flow in the vicinity of the sharp shoulder has been carefully analyzed by studying the locally valid Stokes solution in this region.

Another contribution of the present study lies in the capability developed for determining flows that encounter regions of

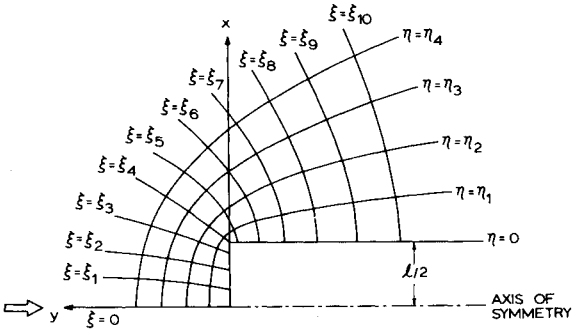

Fig. 1 Semi-infinite body in Cartesian coordinates.

Presented as Paper 74-12 at the AIAA 12th Aerospace Sciences Meeting, Washington, D.C., January 30–February 1, 1974; submitted March 8, 1974; revision received May 31, 1974. This research was supported by the National Science Foundation under Grant GK-35514. The authors are thankful to Prof. M. Van Dyke for his valuable comments and suggestions.

Index categories: Jets, Wakes, and Viscid-Inviscid Flow Interactions; Viscous Nonboundary-Layer Flows.

* Research Assistant Professor, Department of Aerospace Engineering. Member AIAA.

† Professor and Head, Department of Aerospace Engineering. Associate Fellow AIAA.

separation and reattachment. For specified bluntness of the body shoulder, a sufficiently large Reynolds number causes the flow to separate from the surface aft of the body shoulder and reattach to the body surface prior to reaching downstream infinity. This results in a separation bubble of finite, sometimes quite large, size. While the numerical scheme does experience a retardation in its convergence rate for the separated flow cases, it encounters no other difficulty whatsoever. Since the computational domain encompasses the entire flowfield, and not just the separation region as was done by Briley,[5] it has been possible to specify the problem boundary conditions very accurately. To the best knowledge of the authors, this work is perhaps the first of its kind in the Navier-Stokes solutions for flow past semi-infinite bodies including a separation region. It should constitute a firm basis for comparison and assessment of other approximate solutions to such flows, the approximations resulting from simplification of the Navier-Stokes equations.

II. Analysis and Mathematical Formulation

The geometry of the flow considered is shown in Cartesian coordinates in Fig. 1. In this figure, if $l/2$ is taken to represent one unit, then η_1, η_2, η_3, and η_4 correspond to the values 0.25, 0.50, 0.75 and 1.0, respectively. The ξ-coordinate lines are also drawn at ξ increments of 0.25. The complete Navier-Stokes equations are used to describe this laminar incompressible flow. In view of the symmetry about the y axis, it is sufficient to compute the solution in only the upper half of the (x, y) plane. However, for a body with a rounded shoulder, the body surface does not lie along one of the (x, y) coordinate surfaces. Therefore, the body is transformed to a new plane of coordinates (ξ, η), using the Schwarz-Christoffel transformation, such that

$$dz/d\zeta = [Re - \zeta^2]^{1/2} \tag{1}$$

where $z = x + iy$ and $\zeta = \xi + i\eta$. The coordinates x and y have been made dimensionless with respect to the viscous length ν/U_∞ where ν is the kinematic viscosity of the fluid and U_∞ is the undisturbed freestream velocity. The Reynolds number Re has been defined as $Re = (2/\pi)U_\infty l/\nu$ where l is the thickness of the corresponding body with a sharp shoulder. Integration of Eq. (1) yields

$$z = \tfrac{1}{2}\{\zeta(Re - \zeta^2)^{1/2} + Re \sin^{-1}[\zeta/(Re)^{1/2}]\} \tag{2}$$

The transformation defined by Eq. (2) places the body surface along the coordinate surface $\eta = \text{const}$, denoted as η_w, as shown in Fig. 2. This results in facilitating the specification of the boundary conditions of the problem, in addition to leading to certain other advantages which will become clear in the course of the paper. Thus, η_w and Re comprise the two parameters of the problem. Suitable combinations of these parameters allow the study of flow past various geometries as summarized in Table 1 below.

Table 1 Combinations of parameters η_w and Re

	$Re = 0$	$Re \neq 0$
$\eta_w = 0$	Thin flat plate	Rectangular slabs with sharp shoulders
$\eta_w \neq 0$	Parabolic cylinders	Bodies with blunted shoulders
$\eta_w \to \infty$	Infinite vertical wall	

Therefore, the class of symmetric semi-infinite bodies analyzed in the present study includes, as a special case, the family of parabolic cylinders as well as the thin flat plate analyzed elsewhere [Davis,[1] Dennis, and Walsh,[6] and Van de Vooren and Dijkstra[7]].

The transformation defined by Eq. (2) is recognized to be a conformal transformation. Therefore, the scale factors $\bar{h}_1$ and $\bar{h}_2$ of the transformation are given as

$$\bar{h}_1 = \bar{h}_2 = |dz/d\zeta| \tag{3}$$

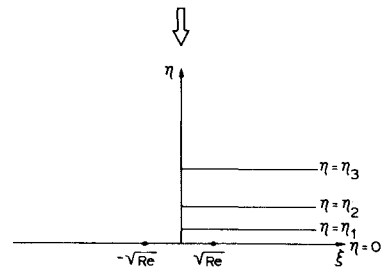

Fig. 2 Semi-infinite body in (ξ, η) coordinates.

Using Eq. (1) and performing the necessary algebra, it can be shown that

$$H^4 = \frac{1}{(\xi^2 + \eta^2 - Re)^2 + 4Re\eta^2} \tag{4}$$

where $H = 1/\bar{h}$ and $\bar{h} = \bar{h}_1 = \bar{h}_2$. The Navier-Stokes equations are now written in terms of these new coordinates using similarity-type variables for the stream function and the vorticity.

Navier-Stokes Equations in Conformal Coordinates and Similarity-Type Variables

The nondimensional form of the unsteady Navier-Stokes equations in terms of the stream function $\psi(\xi, \eta)$ and the vorticity $\omega(\xi, \eta)$ can be written as

$$\psi_{\eta\eta} + \psi_{\xi\xi} = -(1/H^2)\omega \tag{5}$$

and

$$\omega_{\eta\eta} + \omega_{\xi\xi} + \psi_\xi \omega_\eta - \psi_\eta \omega_\xi = (1/H^2)\omega_t \tag{6}$$

where ψ and ω have been made dimensionless with respect to ν and ${U_\infty}^2/\nu$, respectively. The time t has been nondimensionalized by $\nu/{U_\infty}^2$.

Similarity forms are now derived for the stream function and the vorticity. In terms of the (ξ, η) coordinates, the corresponding inviscid flow is the stagnation flow against a vertical wall. It can easily be shown that if it is assumed that the first-order inviscid stream function is of the form $\xi(\eta - \eta_w)$ and the flow due to displacement thickness is of the form $c\xi$, then the optimal coordinates that are orthogonal must necessarily be conformal. The stream function ψ_i for this inviscid flow is obtained as

$$\psi_i = \xi(\eta - \eta_w) \tag{7}$$

Therefore, the suitable form for the stream function of the viscous solution is taken to be

$$\psi = \xi f(\xi, \eta) \tag{8}$$

Substitution of Eq. (8) into the stream function Eq. (5) results in the equation for the new stream function variable $f(\xi, \eta)$ as

$$f_{\eta\eta} + f_{\xi\xi} + (2/\xi)f_\xi = -(1/\xi H^2)\omega \tag{9}$$

The form of the right-hand side of Eq. (9) leads to the following definition for the new vorticity function $g(\xi, \eta)$ as

$$\omega = -\xi H^2 g(\xi, \eta) \tag{10}$$

so that Eq. (9) now becomes

$$f_{\eta\eta} + f_{\xi\xi} + (2/\xi)f_\xi = g \tag{11}$$

Using Eq. (10) in the vorticity, Eq. (6) yields, after some algebra, the transformed vorticity equation as

$$\begin{aligned} &g_{\eta\eta} + [4(H_\eta/H) + \\ &+ \left[\frac{4}{\xi}\frac{H_\xi}{H} + 2\left(\frac{H_\eta^2 + H_\xi^2}{H^2} + \frac{H_{\eta\eta} + H_{\xi\xi}}{H}\right)\right. \\ &\left. + 2\frac{H_\eta}{H}(f + \xi f_\xi) - f_\eta\left(1 + 2\xi\frac{H_\xi}{H}\right)\right] g \\ &+ [4(H_\xi/H) - \xi f_\eta]g_\xi + g_{\xi\xi} + (2/\xi)g_\xi \\ &= (1/H^2)g_t \end{aligned} \tag{12}$$

In terms of the new stream function $f(\xi,\eta)$, the velocity components u and v along the ξ and η directions, respectively, are obtained as

$$u = \xi H f_\eta \tag{13}$$

and

$$v = -H[\xi f_\xi + f] \tag{14}$$

Equations (11) and (12) are the Navier-Stokes equations in terms of the new variables. It is important to note that, as Re approaches zero, the transformation defined by Eq. (2) yields the parabolic coordinates which are known to be the optimal coordinates for the boundary-layer flow past a thin semi-infinite flat plate.[8] This implies that, if the boundary-layer equations are derived directly in the (ξ,η) coordinates, they yield a uniformly valid solution for all η for the thin flat-plate problem. This happens because the boundary-layer solution in optimal coordinates approaches the correct outer flow including displacement effects. Since the thin flat plate represents a limiting case of the body in the present study, it is expected that the coordinates defined by Eq. (2) should also be advantageous for the present problem.

Boundary Conditions and Asymptotic Forms

The surface boundary conditions correspond to the absence of slip at a solid wall, so that

$$f(\xi,\eta_w) = 0 \tag{15}$$

and

$$f_\eta(\xi,\eta_w) = 0 \tag{16}$$

Asymptotically far from the body surface, the external inviscid flow prevails, leading to the boundary conditions

$$f_\eta(\xi,\infty) \to 1 \tag{17}$$

and

$$g(\xi,\infty) \to 0 \tag{18}$$

The symmetry of the flow about the line $\xi = 0$ is used to provide the special forms of the Navier-Stokes equations (11) and (12) valid at this symmetry line.

Finally, at an asymptotically large distance downstream, the Navier-Stokes equations can be shown to reduce to

$$f'' = g \tag{19}$$

and

$$g'' + fg' - f'\{1 + \lim_{\xi\to\infty}[2\xi(H_\xi/H)]\}g = 0 \tag{20}$$

where the primes denote differentiation with respect to η. For the form of H defined by Eq. (4), Eqs. (19) and (20) can be combined and integrated once to yield the familiar Blasius equation. This is exactly what should occur because, as $\xi \to \infty$, the flow past the present body should asymptotically approach the Blasius flow far downstream. Solution of Eqs. (19) and (20) therefore provides the correct downstream boundary condition for the general Navier-Stokes Equations (11) and (12). It should be noted that the correct asymptotic form is also obtained for the case when the surface slope at downstream infinity is a nonzero constant. In this case, Eqs. (19) and (20) will integrate to yield the Falkner-Skan equation where the inviscid surface pressure gradient parameter β_i is to be defined as

$$\beta_i = 1 + \lim_{\xi\to\infty}[\xi(H_\xi/H)] \tag{21}$$

Calculation of Surface Pressure

After the stream function $f(\xi,\eta)$ and the vorticity function $g(\xi,\eta)$ have been determined from a solution of Eqs. (11) and (12), the pressure on the body surface at $\eta = \eta_w$ can be calculated by numerical integration of the momentum equation for the ξ direction. Expressed in terms of the variables f and g, the ξ-direction momentum equation yields an expression for the tangential pressure gradient as

$$\frac{1}{\xi H^2}\frac{\partial P}{\partial \xi} = g_\eta + 2\frac{H_\eta}{H}g + [\xi f_\xi + f]f_{\eta\eta} - \xi f_\eta f_{\xi\eta} - \left[1 + \xi\frac{H_\xi}{H}\right]f_\eta^2 - \frac{1}{\xi}\frac{H_\xi}{H}[\xi f_\xi + f]^2 \tag{22}$$

where the dimensionless pressure variable P has been defined in terms of the dimensional pressure P^* as $P = (P^* - P_\infty)/\rho U_\infty^2$. Using the surface boundary conditions (15) and (16), Eq. (22) yields the surface pressure gradient

$$\left.\frac{1}{\xi H^2}\frac{\partial P}{\partial \xi}\right|_{\eta=\eta_w} = \left.\left[g_\eta + 2\frac{H_\eta}{H}g\right]\right|_{\eta=\eta_w} \tag{23}$$

Equation (22) can also be used to obtain the tangential pressure gradient for the outer inviscid flow by employing in it the conditions for the inviscid flow, i.e., $f = (\eta - \eta_w)$ and $g \equiv 0$, to get

$$\frac{1}{\xi H^2}\frac{\partial P_i}{\partial \xi} = -\left[1 + \xi\frac{H_\xi}{H}\right] - \frac{1}{\xi}\frac{H_\xi}{H}(\eta - \eta_w)^2 \tag{24}$$

where P_i denotes the nondimensional pressure for the inviscid flow. Comparison of Eqs. (21) and (24) shows that, consistent with the present formulation, a general similarity form for the pressure gradient parameter β can be written as

$$\beta = -(1/\xi H^2)\partial P/\partial \xi \tag{25}$$

The surface pressure is evaluated by integrating Eq. (23) backward from downstream infinity where the starting value $P = 0$ is known.

This completes the mathematical formulation of the problem. Before proceeding with the numerical solution, it is of significance to note that the analysis presented in Sec. II is completely general and is valid for any laminar incompressible flow that can be transformed, by a conformal transformation, to the stagnation flow against a vertical wall.

III. Numerical Method of Solution

An alternating direction implicit (ADI) method is used to compute the numerical solution of the governing differential equations (11) and (12) derived in Sec. II. The method is similar to that used in earlier studies by the authors and their co-workers for flows past parabolas and wedges. Therefore, the numerical scheme is outlined here only briefly with respect to the present general formulation which, in fact, encompasses the earlier problems of the parabolas and the blunted wedges.

First of all, it is noted that the steady-state solution is obtained as the asymptotic solution, for large time, of the unsteady governing equations. Since the true transient solution is not of interest here, certain steps are taken to enhance the convergence of the solution to steady state, although these steps cause the transient solution to lose physical significance. These steps include setting to unity the coefficient of $\partial g/\partial t$ in Eq. (12), including a fictitious time derivative term $\partial f/\partial v$ in the stream function Eq. (11) and iterating this equation only once, rather than relaxing it completely, during each time step of the vorticity equation (12). Faster convergence is also achieved by starting the solution with a good set of initial conditions obtained as the numerical solution of the reduced equations that result by neglecting the time derivative terms and the streamwise diffusion terms in the complete governing equations. These reduced equations may be termed the 'parabolized Navier-Stokes equations' because they are the Navier-Stokes equations neglecting the nonparabolic terms. They include all the classical boundary-layer terms as well as the second-order curvature terms.

During a half-step of the ADI scheme used to advance the numerical solution in time, the governing equations (11) and (12) are represented as follows, where the time-derivative $\partial f/\partial v$

has been included on the right-hand side of the stream function equation

$$f_{\eta\eta}{}^{*}-(2/\Delta v)f^{*}-g^{*}=-(2/\Delta v)f_{j+1/2}-[f_{\xi\xi}+(2/\xi)f_{\xi}]_{j+1/2} \tag{26}$$

and

$$g_{\eta\eta}{}^{*}+[4H_{\eta}/H+f^{*}+\xi f_{\xi}{}^{*}]g_{\eta}{}^{*}+\left[\frac{4}{\xi}\frac{H_{\xi}}{H}+2\left(\frac{H_{\eta}{}^{2}+H_{\xi}{}^{2}}{H^{2}}+\frac{H_{\eta\eta}+H_{\xi\xi}}{H}\right)+2\frac{H_{\eta}}{H}(f^{*}+\xi f_{\xi}{}^{*})-\left(1+2\xi\frac{H_{\xi}}{H}\right)f_{\eta}{}^{*}\right]g^{*}+\left[4\frac{H_{\xi}}{H}-\xi f_{\eta}{}^{*}\right]g_{\xi}{}^{*}-\frac{2}{\Delta t}g^{*}=-\frac{2}{\Delta t}g_{j+1/2}-\left[g_{\xi\xi}+\frac{2}{\xi}g_{\xi}\right]_{j+1/2} \tag{27}$$

Considering the $(j+\frac{1}{2})$ subscripted terms as known from a preceding step calculation, Eqs. (26) and (27) comprise a system of partial differential equations, in f^{*} and g^{*}, parabolic in the ξ direction. These can be readily solved along lines of constant ξ, by the implicit numerical scheme developed by Blottner and Flügge-Lotz[9] for the boundary-layer equations using second-order accurate central differences for all η derivatives and a two-point backward difference for the term $g_{\xi}{}^{*}$. It is noted here that the initial condition or the starting solution for the problem is obtained in exactly this manner after neglecting from Eqs. (26) and (27) all their right-hand side terms as well as the terms $(2/\Delta t)f^{*}$ and $(2/\Delta t)g^{*}$ from their left-hand sides.

The next half of the time step in the ADI scheme solves the equations implicitly along lines of constant η. The governing equations (11) and (12) for this half step are written in the following form:

$$[f_{\xi\xi}+(2/\xi)f_{\xi}]_{j+1/2}-(2/\Delta v)f_{j+1/2}=-(2/\Delta v)f^{*}-f_{\eta\eta}{}^{*}+g^{*} \tag{28}$$

and

$$[g_{\xi\xi}+(2/\xi)g_{\xi}]_{j+1/2}-(2/\Delta t)g_{j+1/2}=-g_{\eta\eta}{}^{*}-[4H_{\eta}/H+f^{*}+\xi f_{\xi}{}^{*}]g_{\eta}{}^{*}-\left[\frac{4}{\xi}\frac{H_{\xi}}{H}+2\left(\frac{H_{\eta}{}^{2}+H_{\xi}{}^{2}}{H^{2}}+\frac{H_{\eta\eta}+H_{\xi\xi}}{H}\right)+2\frac{H_{\eta}}{H}(f^{*}+\xi f_{\xi}{}^{*})-\left(1+2\xi\frac{H_{\xi}}{H}\right)f_{\eta}{}^{*}\right]g^{*}-[4H_{\xi}/H-\xi f_{\eta}{}^{*}]g_{\xi}{}^{*}-(2/\Delta t)g^{*} \tag{29}$$

In Eqs. (28) and (29), the $(j+\frac{1}{2})$-subscripted terms are the unknowns whereas the *-superscripted terms are considered known. Use of central differences for all ξ derivatives on the left-hand side of these equations results, again, in a tridiagonal system of equations along lines of constant η; these are solved by the Thomas[10] algorithm.

The solution proceeds alternatively through the * step and the $(j+\frac{1}{2})$ step until the steady-state solution is attained.

Finally, it is recognized that the stream function decays only algebraically to its asymptotic value for large η. This necessitates the outer boundary condition (17) to be imposed only as $\eta\to\infty$. However, it is computationally impractical to work with infinitely large numbers. Therefore, for purposes of the numerical solution, some further transformations must be defined. The new stream function variable used is

$$h=f-\eta \tag{30}$$

so that h remains bounded everywhere. Based on the asymptotic behavior of the flow variables for large ξ and large η, the new independent coordinates are defined as

$$S=1-(A/\xi)\ln[1+(\xi/A)] \tag{31}$$

and

$$N=\frac{\eta-\eta_{w}}{C+(\eta-\eta_{w})} \tag{32}$$

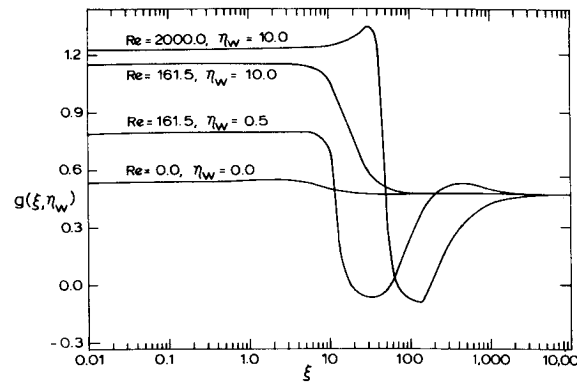

Fig. 3 Vorticity function distribution on surface of blunt-shouldered bodies.

The constants A and C appearing in Eqs. (31) and (32) are chosen so as to obtain a reasonably smooth variation of the vorticity function in the S and N directions, respectively. In terms of the (S, N) variables, the computational region is now bounded in (0, 1) in both coordinate directions. Also, as $\eta\to\infty$, $h_{\eta}\to 0$, in view of the boundary condition (17). The computer program is written using these new variables.

IV. Results and Discussion

Results have been obtained for the stream function, the vorticity function and the surface pressure for several values of the parameters η_w and Re for the flow past the semi-infinite bodies considered. The limiting cases of the parabolic cylinders and the thin flat plate were solved first in order to obtain comparison checks with the results obtained earlier by Davis.[1] These checks show that the solutions presently obtained are indistinguishable from the results of Davis.[1]

The streamwise distribution of the surface vorticity function $g(\xi,\eta_w)$ is shown in Fig. 3 for some typical cases of the body with blunted shoulders. The physical vorticity at the surface is then obtainable as $-\xi H^{2}(\xi,\eta_w)g(\xi,\eta_w)$. For the case with $Re=161.5$, $\eta_w=10.0$, the $g(\xi,\eta_w)$ function decreases monotonically from its leading edge value to the correct Blasius value of 0.470. As η_w is reduced from 10.0 to 0.5, i.e., as the body shoulder is made considerably less blunt, while the Reynolds number is retained at $Re=161.5$, the vorticity function is seen to become negative over an appreciable distance aft of the region of the blunted shoulder. While the drop of the vorticity function to negative values is monotonic, the rise in the skin friction from these negative values to the asymptotic Blasius value is not monotonic. If η_w is retained at its earlier value of 10.0 while the Reynolds number is increased from 161.5 to 2000.0, the flow is again seen to separate in a region beyond the shoulder. For this case, the decrease in the vorticity function from its leading edge value to the negative value in the separation region is not monotonic. However, the behavior of the skin-friction function is seen to be consistent with the accompanying surface pressure distributions for both of these cases. It is also observed from Fig. 3 that as η_w or Re increase, the leading edge value $g(0,\eta_w)$ of the vorticity function approaches the stagnation point value of 1.233. This is because an increase in η_w or Re implies that the shoulder becomes further removed from the point $(0,\eta_w)$ so that its influence on the flow at $(0,\eta_w)$ diminishes. The body presents a leading vertical surface, of increasing extent, to the oncoming stream, causing the flow in the vicinity of the point $(0,\eta_w)$ to approach the stagnation flow.

Figure 4 shows the curves of constant $\eta_w/(Re)^{1/2}$, near the stagnation region, for the parameters η_w and Re having the values used above. These curves provide a representation of the shape of the corresponding body, especially the bluntness at the body shoulder. A change in the values of η_w and Re, such that the ratio $\eta_w/(Re)^{1/2}$ remains fixed, corresponds to a

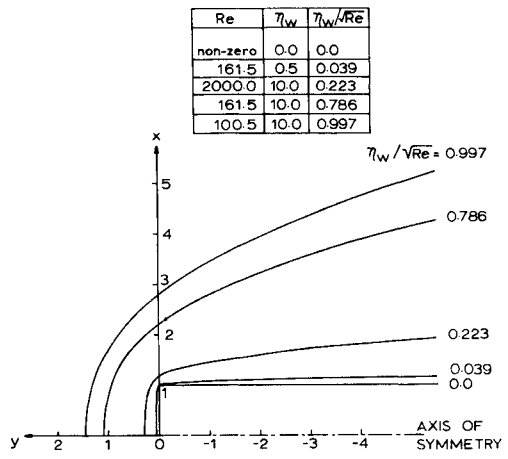

Fig. 4 Typical curves of constant $\eta_w/(Re)^{1/2}$.

change in the actual size of the body, while the body shape is retained to be similar.

The distribution of $g(\xi, \eta_w)$ for the bodies with sharp shoulders is shown by the curves in Fig. 5 plotted $\xi/(Re)^{1/2}$ as the abscissa, so that the sharp shoulder is located at $\xi/(Re)^{1/2} = 1.0$ for all values of the Reynolds number. The values of Re used are such that a grid point is always placed at $\xi = (Re)^{1/2}$ in the finite-difference solution of the problem. This ensures that the sharp shoulder is retained even in the discretized problem. For $Re = 100.5$, the vorticity function is seen to approach extremely close to zero, so that the flow must be on the verge of separation. As Re increases to 161.5 and beyond, the flow is seen to separate aft of the shoulder and reattaches to the plate surface before reaching downstream infinity, leading to a closed separation bubble that increases in extent as Re is increased up to 436.7. However, a further increase in the value of the Reynolds number to 757.8 causes the size of the separation bubble to start reducing, thus indicating that the bubble size probably remains finite for all Reynolds numbers. The smooth approach of the solution to the asymptotic Blasius solution indicates that the Blasius result is the correct asymptotic boundary condition for this flow.

In all cases investigated so far, the flow negotiates the turn around the shoulder without separating. This is confirmed, for large Reynolds numbers, by the locally valid Stokes solution. For large Re, the flow in the vicinity of the shoulder can be viewed as the antisymmetric flow around a corner with reference to a polar coordinate system as shown in Fig. 6. It must be recalled that the Reynolds number here is based on the thickness

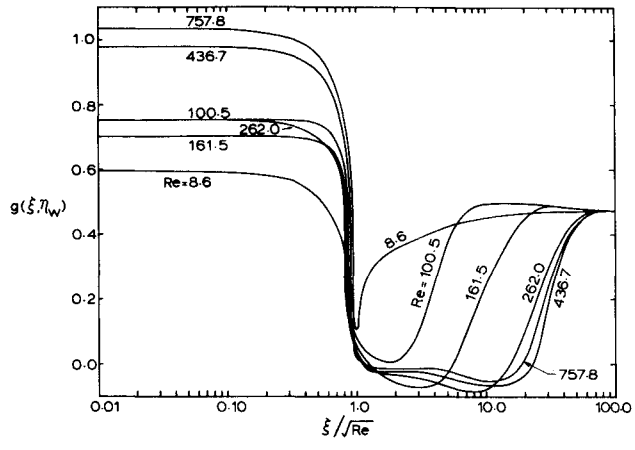

Fig. 5 Vorticity function distribution on surface of thick plates, $\eta_w = 0$.

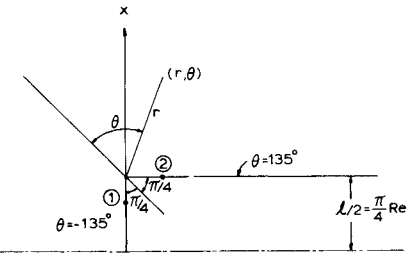

Fig. 6 Polar coordinates and nomenclature for Stokes solution at sharp shoulder.

of the sharp-shouldered plate and is not to be confused with the Reynolds number definitions useful for the Stokes solution. Then, the Stokes stream function $\psi_s(r, \theta)$, valid in the vicinity of the sharp shoulder, for large Re, is governed by the biharmonic equation in (r, θ) coordinates, subject to the boundary conditions of no slip on the solid wall and antisymmetry about the line $\theta = 0$. Accordingly (see Lugt and Schwiderski[11]),

$$\psi_s(r, \theta) = Dr^m\left[\cos(m-2)\theta - \frac{\cos(m-2)(\pi-\delta)}{\cos m(\pi-\delta)}\cos m\theta\right] \tag{33}$$

where $\delta = \pi/4$ for the present problem, $m = 1.5448$, and D is a coefficient to be determined by matching the Stokes solution with the numerically obtained Navier-Stokes solution in the vicinity of the sharp shoulder. Equation (33) leads to the vorticity

$$\omega_s(r, \theta) = -4D(m-1)r^{m-2}\cos(m-2)\theta \tag{34}$$

and the Stokes pressure, except for an additive constant, is obtained as

$$P_s(r, \theta) = -4D(m-1)r^{m-2}\sin(m-2)\theta \tag{35}$$

Clearly, since $m < 2$, both ω_s and P_s become unbounded at the sharp shoulder where $r = 0$. It can be shown, however, that the vorticity given by Eq. (34) leads to a bounded value for the vorticity function $g(\xi, \eta)$ used in the present formulation; in fact, g goes to zero at the sharp shoulder. Since the surface corresponds to $\theta = -135°$ for $\xi < (Re)^{1/2}$ and to $\theta = +135°$ for $\xi > (Re)^{1/2}$, it is clear from Eq. (34) that the vorticity function g does not undergo a change of sign across the sharp shoulder. On the other hand, as seen from Eq. (35), a pressure differential should experience a change in its sign across the sharp shoulder, although the pressure itself may not reveal the change in sign if a sufficiently large value of the additive constant is used. All these characteristics of this local Stokes solution are observed in the numerical results computed. The vanishing value of the vorticity function g at the sharp shoulder, for increasing Re, is most clearly seen for the sharp-shouldered slab with $Re = 8.61$ for which the flow is nowhere near separation.

The results for surface pressure distribution are shown plotted in Fig. 7. In view of the discontinuity in the pressure differential

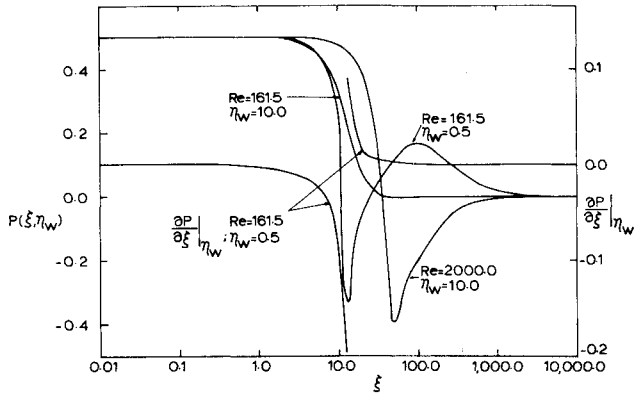

Fig. 7 Surface pressure and surface pressure gradient distributions.

at the sharp shoulder, as discussed above, it is recognized that a unidirectional integration of the surface pressure gradient $\partial P/\partial\xi$ will lead to inaccuracies in the surface pressure values after the shoulder has been crossed. Thus, for the bodies with $\eta_w \ll (Re)^{1/2}$, a backward integration of $\partial P/\partial\xi$, starting from downstream infinity, should be used for $\xi > (Re)^{1/2}$ and a forward integration of $\partial P/\partial\xi$, starting at $\xi = 0$, must be employed for $\xi < (Re)^{1/2}$ in order to obtain accurate values of the pressure on the entire surface. The boundary condition needed at $\xi = 0$ for the forward integration of $\partial P/\partial\xi$ is obtained as the value of the pressure at ($\xi = 0$, $\eta = \eta_w$) determined from integrating the following η-direction momentum equation along the line $\xi = 0$, starting at $\eta \to \infty$, where $P = 0$

$$\left.\frac{\partial P}{\partial \eta}\right|_{\xi=0} = \left[fH(f_\eta H + fH_\eta) - H^2 g\right]\Big|_{\xi=0} \tag{36}$$

A typical curve of the surface pressure gradient is also included in Fig. 6 and shows that the numerical results are in accordance with the analytical predictions [Eq. (35)] for the flow in the vicinity of the sharp shoulder, when Re is large.

For $Re = 161.5$ and $\eta_w = 10.0$, no reverse flow occurs and the pressure decreases monotonically from its leading edge value of about 0.5 to its downstream asymptotic value of zero, the drop occurring mainly in the region of the blunted shoulder. For the cases which encounter a region of separation, the dimensionless pressure decreases to negative values (that is, the dimensional pressure P^* becomes lower than $P_\infty{}^*$) near the shoulder. This is followed by a region of increasing pressure, resulting in the separation of the boundary layer from the body surface. The surface pressure returns to zero further downstream, causing reattachment of the boundary layer.

The value of the pressure difference across the sharp shoulder has also been determined analytically by using the Stokes solution, Eq. (34), at the two points marked "1" and "2" on Fig. 6. These points correspond to the finite-difference computational grid points nearest to the sharp shoulder, on either side of the shoulder, and located on the plate surface. Thus,

$$P_{s,2} - P_{s,1} = -4D(m-1)\sin 3(m-2)\frac{\pi}{4}\left[r_2{}^{m-2} + r_1{}^{m-2}\right] \tag{37}$$

The constant D needed in evaluating $(P_{s,2} - P_{s,1})$ is determined by equating the Stokes vorticity function with the value of g determined numerically from the Navier-Stokes solution. Accordingly,

$$D = \frac{\xi H^2 g}{4(m-1)r^{m-2}\cos(m-2)\theta} \tag{38}$$

evaluated at either point "1" or "2".

The numerical scheme used encounters no difficulty because of the presence of a reversed flow region within the computational domain. Recalling that a backward finite difference has been used for the streamwise convective term g_ξ in the vorticity equation (12), it would appear, at first, that an instability may be encountered for the separated flow cases, in view of the fact that the corresponding boundary-layer formulation does not converge for reversed flow. However, no instability was observed in the present formulation. This is because, although the η implicit sweep in ADI method solves boundary-layer-type equations, the subsequent ξ sweep makes corrections for the upstream influence and displacement effects in the flow. In fact, attempts were made to use a central difference for the convective term g_ξ; obtaining a stable solution by this procedure required a time step at least a hundred times smaller than that usable with the backward difference formulation for g_ξ. Therefore, the backward difference was retained for all cases. For the cases including a separation region, the convergence was markedly retarded; the approach of the solution to steady-state values occurs at a very slow rate. While the cases without separation converged within less than a minute of computing time of the IBM 370/165 computer, some variations could be observed in the results for the separated flow cases even after 10 min of iterations on the same computer. Even though the changes were occurring in the third decimal place, they could become significant if they continue to persist through several more iterations. Some attempts were made to enhance the convergence rate by use of different values of the time steps Δv and Δt in the governing equations, but no particularly optimum time steps have been determined so far.

It is generally acknowledged that the use of upwind differences or directional differencing is advantageous for stability and convergence of the numerical solution because upwind differencing takes into account the direction of the flux of information arriving at a point in the flowfield, while also introducing an artificial viscosity term in the finite-difference equations. However, the use of upwind differences for the present problem leads to negligibly small improvement in the convergence rate as compared to the backward difference formulation for g_ξ. In order to observe the effect of the artificial viscosity term introduced by the use of directional differencing, the equivalent of this term was subtracted from the finite-difference equations. This can be achieved as follows without the use of additional logical "IF" statements in the computer program. Denoting by C_4 the coefficient of the convective term containing g_ξ in Eq. (12), this term is written in finite-difference form as

$$C_4\frac{\partial g}{\partial S}\frac{dS}{d\xi} = -\frac{1}{2}(|C_4| - C_4)\left[\frac{g_m - g_{m-1}}{\Delta S}\right]\frac{dS}{d\xi} - \frac{1}{2}(C_4| + C_4)\left[\frac{g_m - g_{m+1}}{\Delta S}\right]\frac{dS}{d\xi} - \frac{\Delta S}{2}|C_4|\left[\frac{g_{m+1} - 2g_m + g_{m+1}}{(\Delta S)^2}\right]\frac{dS}{d\xi} \tag{39}$$

where

$$C_4 = 4H_\xi/H - \xi f_\eta \tag{40}$$

In Eq. (39), S is the independent variable defined by Eq. (31) and m is the discretized grid counter increasing in the direction of increasing S. The last term on the right-hand side of Eq. (39) represents the correction for the artificial viscosity diffusion term.

For forward flow, $C_4 < 0$ and Eq. (39) replaces g_ξ by a first-order accurate backward difference together with the correction term. In regions of reversed flow, C_4 may become positive. In that case, Eq. (39) replaces g_ξ by a first-order accurate forward difference along with the correction term. A stable solution again required a reduction of the time steps by a factor of at least 100, but the convergence rate remained almost unaltered. This is obvious because the removal of this artificial viscosity term is, in a sense, equivalent to the use of a central difference for the convective term; the latter procedure had been earlier determined to require similar reductions in the time steps. It is worth noting, however, that for unseparated flow, the solution remains almost unaffected by the artificial viscosity term. The corresponding separated flow has not yet been fully resolved using this formulation.

One purpose that the present study can serve is to analyze the question: when and how, if at all, can the boundary-layer equations be used to provide reasonable solutions for separated flow? It has been well established that the boundary-layer equations may be used to predict separated flow if the boundary layer is allowed to continuously interact with the external inviscid flow, thus generating its own true pressure gradient, rather than employing the basic inviscid pressure gradient. In other words, the correct displacement effects must be taken into consideration. For separated flow, the displacement body may not be determined, a priori. However, an accurate method of accounting for displacement effects arises through recognizing that the terms $[f_{\xi\xi} + (2/\xi)f_\xi]$ in the stream function equation correspond essentially to displacement effects. Therefore, in partial answer to the question addressed to above, solutions were obtained by parabolizing the vorticity equation, i.e., neglecting the terms $[g_{\xi\xi} + (2/\xi)g_\xi - g_t]$ in Eq. (12) while retaining the complete stream function equation (11). These results reproduce almost exactly the corresponding solutions of the complete

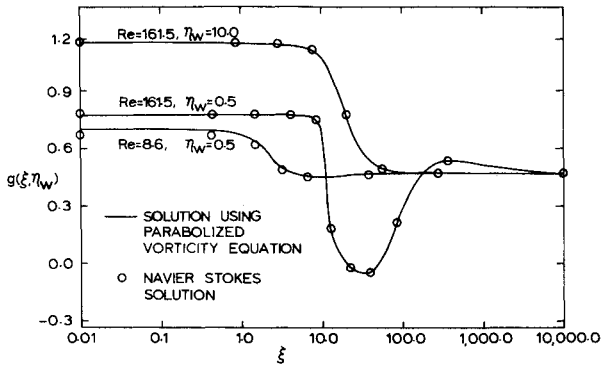

Fig. 8 Surface vorticity function distribution using parabolized vorticity equation.

Navier-Stokes equations for the three cases for $\eta_w = 10.0$ and $\eta_w = 0.5$ as shown in Fig. 8. For the values of η_w shown, the stagnation point skin friction, determined from the two solutions, differs by a maximum of 3.5% for a range of Reynolds numbers between 2.22 and 2000.0. This has the very significant implication that it is not necessary to solve the complete Navier-Stokes equations in these separated flow studies; it is possible to use a considerably simplified form, of the boundary-layer type, for the vorticity equation. This indicates that boundary-layer equations should be adequate for analyzing these separated flow cases if an accurate model is employed for the corresponding inviscid flow.

V. Conclusion

The flow past a class of semi-infinite two-dimensional bodies with blunted or sharp shoulders has been studied using the Navier-Stokes equations. To the best knowledge of the authors, the analysis developed in the present paper is the first of its kind for the body shapes considered. The formulation is quite general and includes the flow past parabolic cylinders, thin flat plates and vertical walls as special cases. Other body shapes (e.g., wedges) could also be easily studied by appropriately redefining the function H in Eq. (4). The flow in the vicinity of the sharp shoulder has been carefully analyzed. While separated flows have been studied by other researchers, as for instance, Briley[5] and Leal,[12] using the Navier-Stokes equations, the present analysis appears to be free of anomalies in the boundary conditions of the problem. Therefore, the results of the present study can lead to assessment and improvements in boundary-layer analysis for separated flows. The good agreement between the Navier-Stokes solution and the results obtained when the vorticity equation was parabolized indicates that it may be possible to study separated flow with boundary-layer-type equations if displacement effects are appropriately taken into consideration.

References

[1] Davis, R. T., "Numerical Solution of the Navier-Stokes Equations for Symmetric Laminar Incompressible Flow Past a Parabola," *Journal of Fluid Mechanics*, Vol. 51, Pt. 3, 1972, pp. 417–433.

[2] Davis, R. T. and Werle, M. J., "Laminar Incompressible Flow past a Paraboloid of Revolution," *AIAA Journal*, Vol. 10, No. 9, Sept. 1972, pp. 1224–1230.

[3] Davis, R. T., Ghia, U., and Ghia, K. N., "Laminar Incompressible Flow Past a Class of Blunted Wedges using the Navier-Stokes Equations," Aerospace Engineering Rept. AFL-73-7-2, 1973, Univ. of Cincinnati, Cincinnati, Ohio; to be published in *International Journal on Computers and Fluids*.

[4] Davis, R. T., Ghia, U., and Ghia, K. N., "Laminar Incompressible Flow past Sharp Wedges," presented at the Symposium on Application of Computers to Fluid Dynamic Analysis and Design, Jan. 1973, Polytechnic Institute of Brooklyn, Brooklyn, N.Y.; *International Journal on Computers and Fluids* (to be published).

[5] Briley, W. R., "A Numerical Study of Laminar Separation Bubbles using the Navier-Stokes Equations," *Journal of Fluid Mechanics*, Vol. 47, Pt. 4, 1971, pp. 713–736.

[6] Dennis, S. C. R. and Walsh, J. D., "Numerical Solutions for Steady Symmetric Viscous Flow Past a Parabolic Cylinder in a Uniform Stream," *Journal of Fluid Mechanics*, Vol. 50, Pt. 4, 1971, pp. 801–814.

[7] Van de Vooren, A. I. and Dijkstra, D., "The Navier-Stokes Solution for Laminar Flow past a Semi-Infinite Flat Plate," *Journal of Engineering Mathematics*, Vol. 4, No. 1, 1970, pp. 9–27.

[8] Kaplun, S., "The Role of Coordinate Systems in Boundary Layer Theory," *ZAMP*, Vol. 5, 1954, pp. 111–135.

[9] Blottner, F. G. and Flügge-Lotz, I., "Finite Difference Computation of the Boundary Layer with Displacement Thickness Interaction," *Journal de Mécanique*, Vol. 2, No. 4, 1963, pp. 397–423.

[10] Thomas, L. H., "Elliptic Problems in Linear Difference Equations over a Network," Watson Science Computing Lab. Rept., 1949, Columbia University, New York.

[11] Lugt, H. J. and Schwiderski, E. W., "Flow around Dihedral Angles, Part I. Eigenmotion Analysis," *Proceedings of the Royal Society of London*, Ser. A, Vol. 285, 1965, pp. 382–399.

[12] Leal, L. G., "Steady Separated Flow in a Linearly Decelerated Free Stream," *Journal of Fluid Mechanics*, Vol. 59, Pt. 3, 1973, pp. 513–535.